Numerical modelling of the yielding of a stabilizing pillar/foundation system and a new design consideration for stabilizing pillar foundations

by G. York*

Synopsis

Following a short review of selected literature, a back analysis of stress measurements of stress regeneration in a closed mini-longwall is shown. The agreement is good, lending confidence to the parameters used in the proposed numerical model. Foundation yielding was modelled in the absence of total stope closure. A 'Prandtl' wedge was formed, coinciding with the yield point of the pillar/foundation system. Some theoretical work is used as a starting point for the formulation of a new design methodology for strike or dip stabilizing pillar/foundation systems in deep level gold mines. The existing guideline for the stability of foundations (APS < 2.5UCS) is critically examined. Finally, the advantages of the new approach, and the work required to substantiate the proposed new design methodology, are outlined.

Introduction

The current design guidelines for the stability of foundations of strike stabilizing pillars state that the average pillar stress (APS) should not exceed 2.5 times the laboratory uniaxial compressive strength (UCS) of intact footwall or hangingwall material, whichever is weaker (Anon, 1988).

This value is based on a series of laboratory tests performed by Wagner and Schümann (1971). Punch tests were performed on five rock types, for punch diameters ranging from 3.8 to 30.5 mm. The steel punches were driven into rock samples of diameter 150 mm and height 100 mm. Wagner and Schümann concluded that, for brittle rocks, the ultimate bearing capacity of the rock under the punch (the 'foundation'), tended to a value of four times the UCS of the foundation as the punch diameter increased. This formed the basis of the guideline for the bearing capacity of foundations under stabilizing pillars: taken as three times the UCS of the foundation material (Ryder, 1997; Anon, 1977). The value was reduced from four to three to account for the lower strength expected for an *in situ* rock mass (Ryder, 1997). This value was lowered to 2.5 in the second edition of the Industry Guide (Anon, 1988), in view of occurrences of foundation failure occurring in the industry at the time, specifically at Western Deep Levels Gold Mine (WDL) (Ryder, 1997).

Lenhardt and Hagan (1990) performed an analysis of seismic events recorded in the foundation of the 109 strike stabilizing pillar at Western Deep Levels—West Mine. The pillar was in the Carbon Leader Reef, at a depth of 3100 m below surface. Using the results shown in Figure 1, Lenhardt and Hagan inferred the following:

- there was a well-defined failure plane approximately perpendicular to the reef plane at the down dip edge of the pillar, in the footwall
- there was a similar but less well-defined failure plane at the up dip edge of the pillar in the footwall
- there was a 'conspicuous' lack of seismic activity in the core of the pillar.

Leach and Lenhardt (1990) noted that the magnitude of pillar related seismic events is unrelated to pillar width (in the range from 20 to 60 m). This was commented on by Lenhardt (1992), who explained that the determining factor in seismic magnitude is the extent of failure along the edge of the pillar. This mechanism leaves the core of the pillar intact. The phenomenon is therefore independent of the width of the pillar. In this regard, Lenhardt postulates that the APS as a pillar design criterion is inadequate. Rather, the shear stresses at the pillar edge should be a design parameter. Lenhardt suggested that numerous case studies be performed to establish the necessary guidelines for this new criterion. Thus far, Lenhardt's proposed design criterion has not been followed up by other researchers.

Handley *et al.*(1997) also found that stabilizing pillar-related seismicity in the back

* *CSIR, Division of Mining Technology, Johannesburg, South Africa, P.O. Box 91230, Auckland Park, 2006.*

© *The South African Institute of Mining and Metallurgy, 1998.* *SA ISSN 0038–223X/3.00 + 0.00. Paper received Jul. 1998; revised paper received Aug. 1998.*

area was not related to the width of the pillar, nor to the dip spans of the stopes supported by the pillar. They did not comment on the relation between pillar width, dip span and seismicity.

Numerical modelling of a stabilizing pillar

The aim of the numerical modelling was to investigate foundation failure mechanisms associated with stabilizing pillars in deep level gold mines. The dimension and rock properties were chosen from Kloof Gold Mine (Kloof) on the West Rand. Complete stope closure occurs at Kloof. A stress measurement was performed in the closed stope under SIMRAC project GAP223. This provided a measurement from which a back analysis could be made.

The numerical modelling, using the FLAC code, reported in this paper assumes an infinite train of repeating pillars in a horizontal reef. The effect of dip on strike stabilizing pillars was thus not evaluated. The effect of ride in the out-of-plane direction on the dip pillars in 'scattered mining with dip pillar' (SMDP) mining layouts is thought to be negligible. FLAC was selected for its ease of use and because it is able to perform non-linear modelling, with localization of shear bands.

The dimensions used in the model were based on typical dimensions at Kloof Gold Mine. Kloof employed a strike stabilizing pillar layout. The stoping width was 1.2 m. The pillar width was 48 m, with a stope span of 272 m, resulting in a pillar centre-to-centre distance of 320 m. The tributary area extraction ratio was 85 per cent. The vertical dimension of the model was based on results shown by Özbay and Ryder (1990). They stated that, at an elevation above the stope equal to the pillar centre-to-centre distance, for repeating pillar geometries, the vertical displacement is uniform, and the vertical stress reverts to virgin stress. Hence the vertical dimension was set to 320 m, with an applied vertical stress equal to the virgin stress of 80 MPa. As shown in Figure 2, quarter symmetry was used.

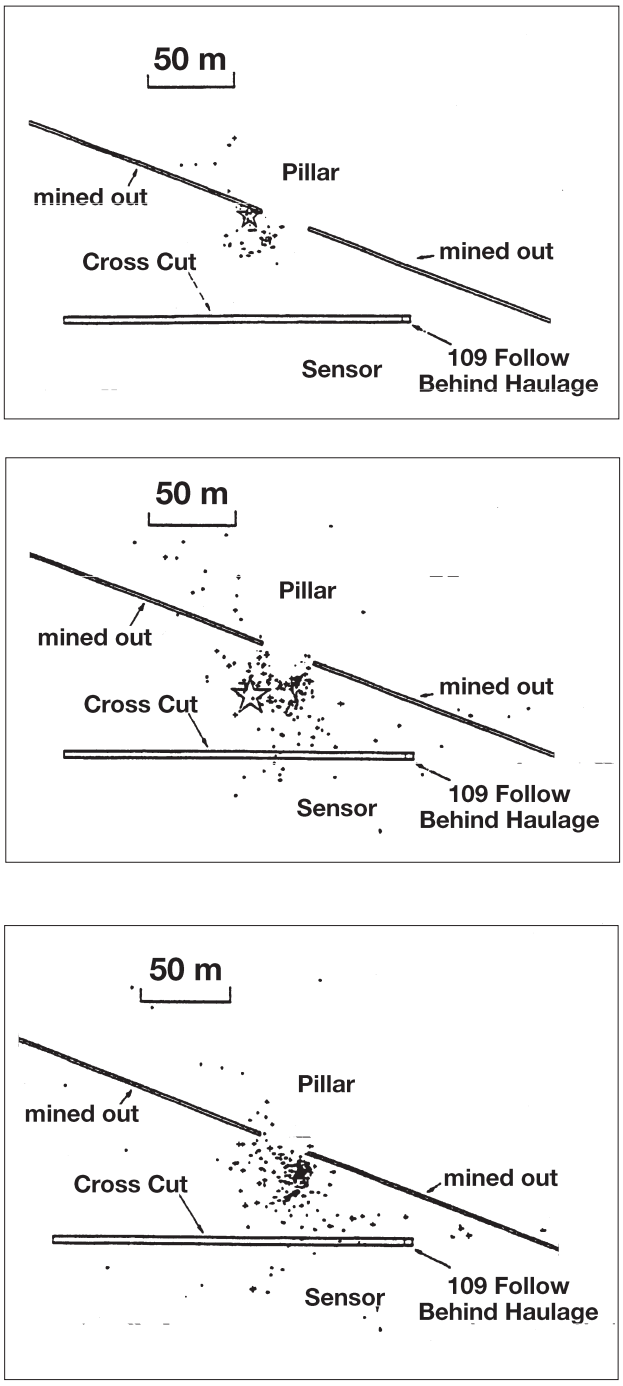

Figure 1—Cross sections showing acoustic emissions associated with a magnitude 3.3 seismic event at WDL (after Lenhardt and Hagan, 1990). The sequence of diagrams shows the foreshocks, the main event, and the aftershocks respectively

Elastic solutions

The depth modelled was just under 3000 m, and a rock mass density of 2700 kg/m^3 was assumed. The elastic constants used in all the modelling were Young's modulus $E = 70.3$ GPa and Poisson's ratio $\nu = 0.22$. The model was checked against the analytic solutions provided by Salamon (1963), for the distribution of vertical stress across the pillar, and for the stope convergence profile. The stope convergence profile predicted by FLAC was less than 1 per cent different from the Salamon solution, except near the pillar edge. The Salamon solution assumes no vertical deformation of the pillar, while FLAC explicitly models such deformation, because the height of the pillar is explicitly modelled. The error in total volumetric convergence was less than 0.7 per cent. The FLAC generated distribution of vertical stresses across the pillar was close to the analytic solution. The errors were significant only near the edge of the pillar. The maximum error occurred near the edge of the pillar, in which the FLAC model underestimated the vertical stress by about 20 per cent. This is again mostly due to the explicit stoping width that is modelled by FLAC. The error in APS was 0.15 per cent.

In addition, the deformation of the pillar system was checked against a result determined by Özbay and Ryder (1990), based on Salamon's solutions for repeating pillars. The average induced vertical displacement is the same across any horizon above or below the stope horizon. This value is equal to the average convergence of the hangingwall, assuming symmetric convergence of the hanging- and footwall. The modelled convergence profiles at horizons 100 and 320 m above the reef horizon (at the top of the model) were checked against this result. The results agreed with the analytic solution with error magnitudes similar to those mentioned above.

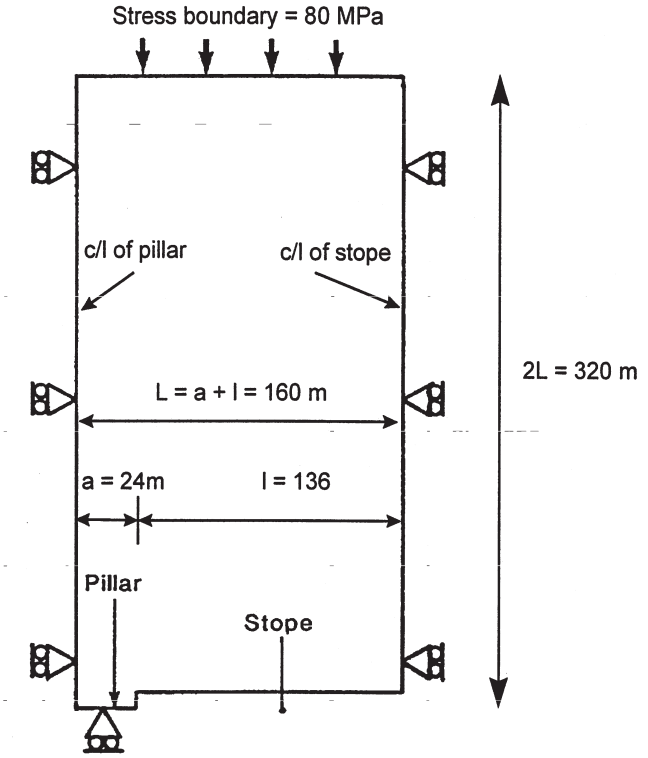

Figure 2—The FLAC two-dimensional plane strain model geometry and boundary conditions

Having established that the model performed correctly, the next step was to model pillar and foundation failure with strain hardening or softening material.

Strain softening parameters

No specific hardening or softening constitutive law was used. A curve fitting exercise was performed, using the program SS written at Miningtek (Ryder, 1994). The program simulates triaxial compression curves, based on user specified values of cohesion, angle of internal friction (friction angle) and dilation. The values of cohesion, friction angle and dilation may change with respect to plastic strain. These relations are specified as parameters in FLAC, to describe the performance of the material. Failure is determined according to the Mohr-Coulomb criterion. Plastic flow is non-associated.

The Mohr-Coulomb cohesion and friction angle were based on a series of tests performed on footwall quartzite from Kloof. The friction angle and cohesion were 39° and 44 MPa respectively. The strain hardening/softening parameters are presented in Table I, where ε^p is the plastic shear strain.

As a check, a series of triaxial tests were simulated in FLAC. The results are shown in Figure 3. The peak strengths predicted by the SS program, as well as the actual laboratory strengths, are also plotted in Figure 3. As can be seen, good agreement is obtained, between:

- The laboratory test results and the predictions by the program SS
- The SS and FLAC predictions.

The 90 MPa data point was generated in the program SS to ensure that the parameters as chosen did not lead to unexpected behaviour at higher confining stresses. The FLAC 90 MPa stress strain curve shows increased ductility compared to the curves for the lower confining stresses, and a lower drop-off in the stress after the peak strength is reached. Qualitatively, this is expected with increased confinement.

Table I

Values of cohesion, friction and dilation angles as functions of plastic strain; as input parameters for use in the FLAC 'strain softening' constitutive model

Cohesion		Friction Angle		Dilation Angle	
ε^p (mε)	cohesion (MPa)	ε^p (mε)	ϕ (°)	ε^p (mε)	dilation angle (°)
0.0	25.4	0.0	21.6	0.0	0.0
0.5	25.4	0.5	34.0	2.0	10.0
1.0	22.6	1.0	37.6	10.0	0.0
4.0	5.4	1.5	40.0		
4.5	3.4	2.0	41.6		
5.0	1.8	2.5	42.4		
5.5	0.8				
6.0	0.4				

Other quantities, such as plastic strains at peak strength, simulated Mohr-Coulomb cohesion and friction angle, and residual strength were also compared, to obtain as good a fit as possible.

The values shown in Table I include two adjustments, for use as material parameters in the numerical modelling. Firstly, due to the requirements for intact/*in situ* strength downgrading and in agreement with the results of Kersten and Leach (1996) in a back analysis of the behaviour of deep level gold mining rock mass, the value of cohesion was halved. Unlike the analysis of Kersten and Leach, the friction parameters are unchanged. The implied UCS thus drops from about 190 MPa shown in Figure 3 to about 95 MPa. The data in the back analysis of Kersten and Leach consisted of deformations of the sidewalls of a tunnel. This is a different

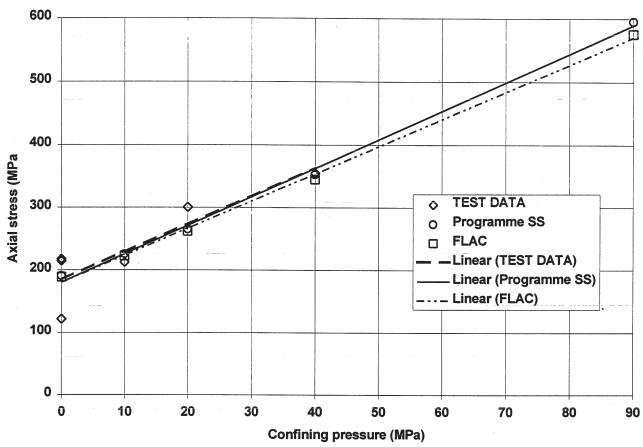

Figure 3—A comparison between the peak strengths of the laboratory test data on footwall quartzite, the values predicted by the SS program, and those predicted by FLAC

stress regime to that of a squat stabilizing pillar and foundation. In a tunnel sidewall, confining pressures are low or close to zero, while the stabilizing pillar is highly compressive, with high confining pressures, akin to triaxial conditions. In a jointed medium, it is the author's opinion that strength reductions occur as a result of reductions in cohesion, rather than the frictional properties of the material.

The second adjustment involved the plastic strains used in the strain hardening/softening model. A laboratory test sample is constrained at the top and bottom due to the frictional contact between the sample and the end pieces. This induces two regions that are effectively more confined than the rest of the sample. This results in much of the damage occurring some distance away from the end pieces, perhaps in the region between the upper and lower quarter of the sample. However, the plastic strains are calculated assuming the full length is equally confined (plastic strains are calculated using the displacement of the loading piston and the change in volume of the confining fluid). As an approximate correction therefore, the plastic strains are doubled.

Modelling methodology

York (1997) describes a methodology whereby the load is transferred to the pillar in a finite number of discrete stages. The model is brought to equilibrium at each stage. This provides two capabilities:

- the model may be investigated at any stage to determine various mechanisms of deformation, failure, etc, related to specific stages in the loading history
- particular stages in the loading history may be related to a distance to the mining face in a three-dimensional sense.

Modelling of complete stope closure

As stated, complete closure occurs in the back areas at Kloof. Major principal stresses (sub-vertical) of about 36 MPa have been measured under the strike centre line of a stope protected by stabilizing pillars by means of the doorstopper technique (Vlietstra, 1995). The measurements were performed at a depth of 2821m, which is close to the simulated depth in the numerical model.

A vertical stress of 36 MPa represents approximately 1300m of overburden. Therefore this stress regeneration cannot be directly due to inelastic skin effects, such as dilation on parting planes. Rather, a significant portion of the overburden load is transmitted through the closed stope. This can only occur if large amounts of inelastic deformation occur in the surrounding rockmass.

During the course of the FLAC numerical simulation, the stope was constantly monitored for total closure by means of a user defined function. The function determines which portion of the stope is closed, and then calculates the average vertical stress in this portion.

As complete stope closure occurs, the load transfer to the pillar reduces, because stress is now transmitted through the stope. This effect is shown in Figure 4. The APS of the pillar flattens as the average stress in the stope increases. In the case modelled, the APS was limited to 379 MPa. In the model, the width of the closed portion of the half span was 89 m, out of a total half span of 136 m. Stress is, therefore, being transmitted through almost two-thirds of the stope span. The average vertical stress in the closed portion of the stope was 39 MPa. About 27 per cent of the overburden load was transmitted through the closed stope, i.e. the pillar is relieved of 27 per cent of the ultimate load it would receive if no total stope closure had occurred. The simulated stress regeneration is close to the *in situ* measured value of 36 MPa, the difference being less than 10 per cent.

The total load transmitted through the pillar and the closed stope must be equal to the total overburden over the pillar and the span before the span was mined. This has the value ql = 80 MPa x 160 m = 12 800 MN/m (where q = virgin vertical stress, and l = half the pillar centre-to-centre distance). The sum of the modelled loads in the closed stope and the pillar was 12 689 MN/m. This is an error of less than one per cent.

The similarity in the values of stope regenerated stresses in the model and *in situ*, provides some confidence in the strain hardening/softening parameters. Confidence is also lent to the failure mechanisms of the model. The failure mechanisms will be discussed in the next section.

The listing of the FLAC data file and user defined functions used for this analysis may be found in the Appendix, under the file name 'ss-ref.d6m'.

Modelling of foundation failure mechanisms

The stoping width was modelled as 3.6m, to avoid stope closure in the model. This, therefore, allows the full overburden load to be transferred to the pillar.

The average pillar stress-average vertical strain curve of the pillar is shown in Figure 5. The straight line is the linear elastic curve. The value of the first yield of the non-linear curve is low compared to the final stress borne by the pillar. Typically, in UCS tests on brittle rock, the yield stress is in the range of 60 to 70 per cent of the strength. In the loading process in the model, a stress concentration is present at the edge of the pillar. The first yield point then, is indicative of failure of the edge of the pillar.

The second yielding point (marked A) corresponds to the yield point of a laboratory UCS test. However, because of the large w/h ratio, this is much higher than the expected value of the yield point of a laboratory UCS test. The well defined yield point is at an APS of 302 MPa, and a pillar strain of 9.2 mε.

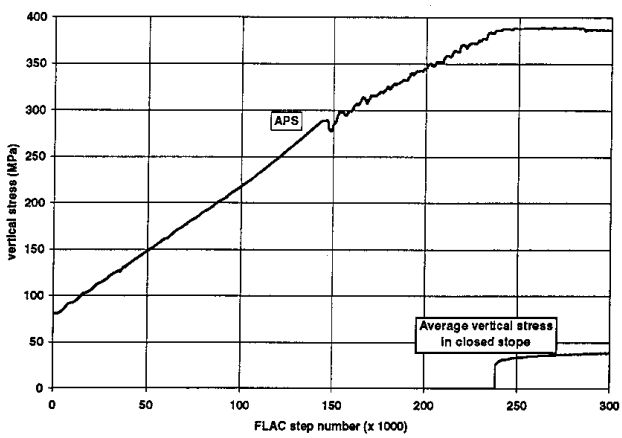

Figure 4—Results of the numerical model of total stope closure, showing the average pillar stress (APS) and the average stress in the closed stope

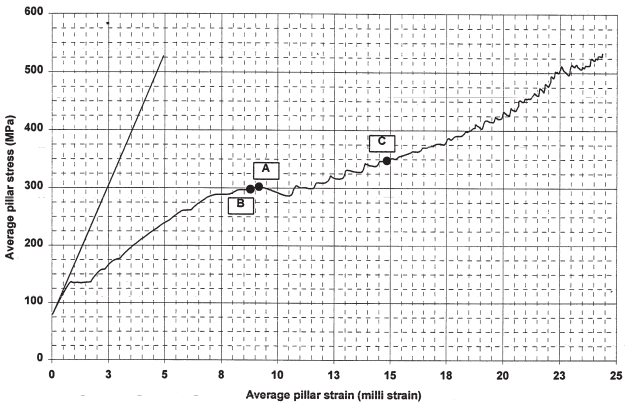

Figure 5—The FLAC simulated stabilizing pillar stress-strain curve

The mechanism of this behaviour can be seen by observing the distribution of vertical displacement and plastic shear strain in the model (Figure 6 and Figure 7), corresponding to points B and C in Figure 5. The pillar is in the bottom left corner of each plot. The contour intervals for vertical displacement are the same for both of the plots (50 mm). In the displacement plot of Figure 6, corresponding to point B, there are no well defined concentrations of displacements. In the displacement plot of Figure 7, corresponding to point C, a plane has developed perpendicular to the reef plane, on which vertical displacement is concentrated. The material in the pillar foundation, bounded by this plane, is relatively intact. It would appear that the pillar/foundation system is 'punching' into the rockmass. This effect becomes more pronounced as more load is transferred to the pillar. The contours are parallel in the 'punch', indicating a laterally uniformly distributed downward compression within the punch. This is similar to the first and third plots of Figure 1. The plastic shear strain plot in Figure 7 shows that the hangingwall has sheared down and around the punch (shown by the grey lines). By contrast, the shear strain shown in Figure 6 has not caused major dislocations in the foundation. There is a sub plane of slip to the right of the main slip plane in Figure 7. The contours of plastic strain show that shear band localization has occurred on these planes. Thus, the foundation yielded on shear bands, so as to allow the pillar to 'punch' into the hangingwall. This shear localization is likely to be a series of rapid events equivalent to seismic events experienced in stabilizing pillar/foundation systems.

Although the foundation seems to be yielding, there is nevertheless a marked decrease in the slope of the stress strain curve of the pillar itself (from point A onwards in Figure 5). This is explained as follows. The vertical strain in the pillar is calculated by taking the average vertical displacement of the grid points that form the pillar/hangingwall contact, divided by half of the stoping width (by means of a user defined function). As stated, the punch is formed by the development of a shear band in the foundation at the effective edge of the pillar. The shearing movement involves a downward movement of the hangingwall at the effective edge of the pillar. The nominal edge of the pillar has by this time already failed. The high stress concentration that may be expected at the edge of the

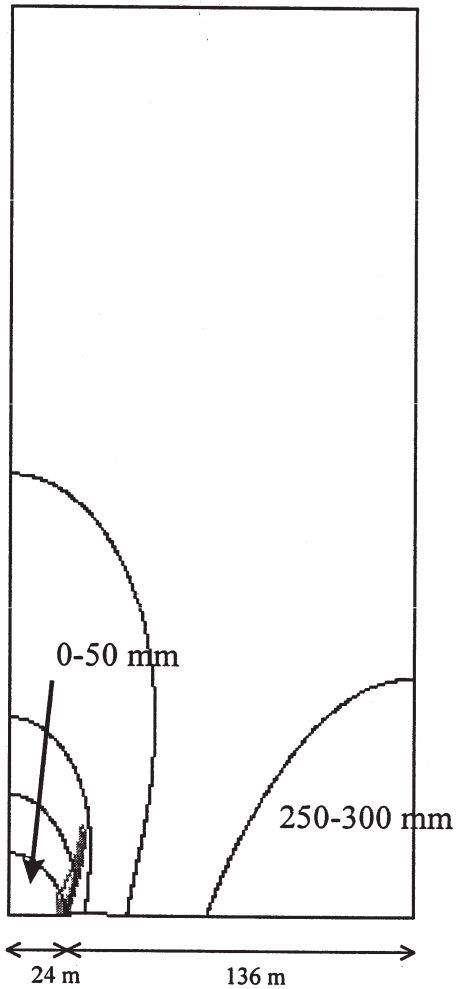

Figure 6—Contours of vertical displacement and total plastic shear strain corresponding to point B in Figure 5

pillar is, therefore, a little way in from the edge of the pillar (the stress peak is 4 m from the edge of the pillar, see Figure 8). The effective half-width of the pillar is thus 20 m, with the 'punching' action acting also across 20 m. The shear localizations at the effective edge of the pillar cause large vertical displacements of the grid points that are nominally in the pillar/hangingwall contact. In addition, even without this shear induced displacement, the draping effect of the closure of the hangingwall, on the edge zones that carry little stress, is such that displacements are increased. The draping effect is likely to be considerably greater underground and in the numerical model, than found in laboratory experiments, as the stiffness of the hangingwall is less than the platens used in typical stiff testing machines. The net effect of these two factors may be seen in Figure 8. There is a sharp increase in the vertical displacement of the grid points near the edge of the pillar. The FLAC j = 1 to j = 6 are the stress profiles in the grid rows from the mid-height of the pillar to the top of the pillar respectively. The stress peak has shifted four metres in from the edge of the pillar. The material between 20 and 24 m dilates significantly.

This agrees with the observations of stress fracturing shown in Figure 9, in which most of the dilation is confined to the first 4 m from the pillar edge, with a tailing off to zero visible open fractures beyond 8 m (Vieira, 1997).

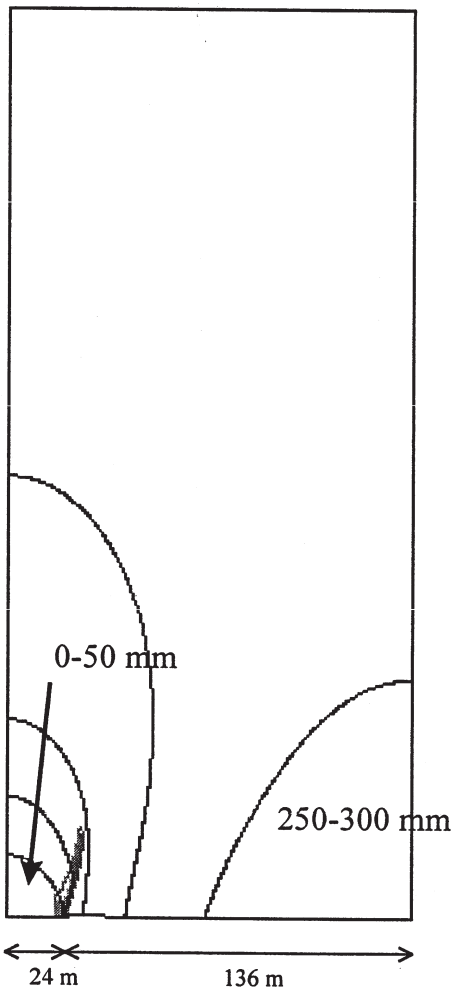

Figure 7—Contours of vertical displacements and total plastic shear strain corresponding to point C in Figure 5

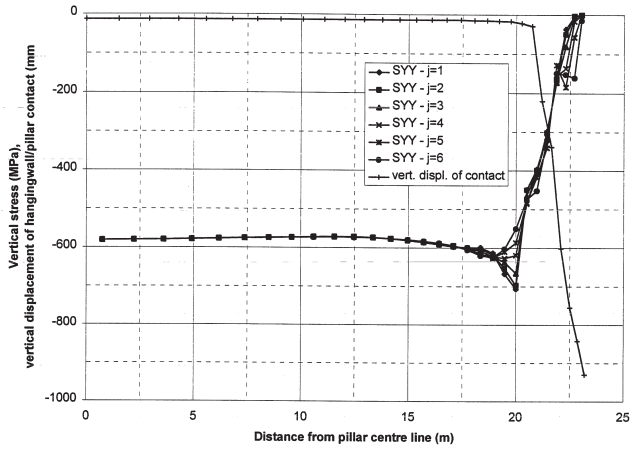

Figure 8—The pillar stress distribution and hangingwall contact displacement distribution after completion of load transfer. The edge of the pillar is at 24 m

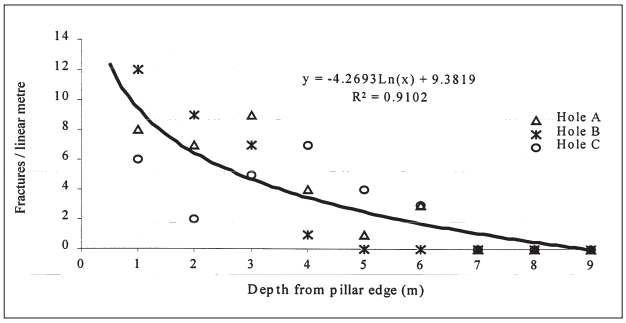

Figure 9—Distribution of induced fracturing in a 45 m wide strike stabilizing pillar at 2200 m below surface, after 4 months of monitoring (after Vieira, 1997)

The overall yielding mechanizm of the pillar system is thus a linked two-staged process in which a shear band localization leads to the formation of a punch in the foundation. This foundation yielding causes large vertical movements just inside the edge of the pillar, above the failed material at the edge of the pillar. This causes the strain value to increase rapidly, defining the yield point in Figure 5.

At the completion of load transfer onto the pillar, a well defined wedge shaped 'punch' has formed, as shown by the plot of vertical displacements in Figure 10 (a 90 by 90 m window is shown, with the 24 m wide half pillar at the bottom left). The plastic shear strain rate, which is the current strain applied in the model, shows that at the end of the load transfer process, shear movement is concentrated along the boundary of the wedge (Figure 11, with the same window as Figure 10). The stress state in the wedge is effectively hydrostatic. This agrees with the discussion by Cook *et al.* (1984), and with the solutions presented by Prandtl (1920).

The displacement of the top boundary may be regarded as the regional displacement, because the vertical displacement of the top boundary is uniform (Özbay and Ryder, 1990). The regional closure rate (Figure 12) also shows an increase at an APS that corresponds to the yield point shown in Figure 5. This indicates that the regional closure rate also increases upon the formation of the wedge. The formation of the wedge, therefore, allows the whole hangingwall to shear downwards relative to the 'punch', almost in a rigid block fashion.

Using the methodology described by York (1997), the distance to face at which yield of the foundation occurred was determined as 65 m. This agrees well with the distances to face quoted by Lenhardt and Hagan (1990), who found that pillar associated seismicity trailed the face by a distance ranging from 65 to about 95 m. Despite the large 'regional' inelastic movements, the condition at the top boundary (viz. that the vertical displacement is uniform across this elevation) in the model was not compromised.

This increased regional closure rate also explains how the effectiveness of stabilizing pillars in controlling the energy release rate (ERR) on longwall faces is reduced. Conditions at the face are likely to worsen as the regional closure increases, i.e. the further beyond the yield point the foundations are. The methodology to quantify these effects was developed by Özbay and Ryder (1990), and further developed by York (1997). An application of the methodology is shown by York (1997).

The listing of the FLAC data file and user-defined functions used for this analysis may be found in the Appendix, under the file name 'ss-ref.d6k'.

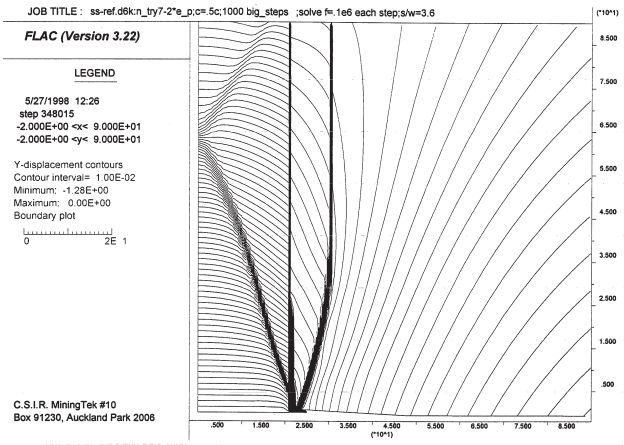

Figure 10—Contours of vertical displacement at ultimate load. A 90 by 90 m window is shown, with the 24 m wide half pillar at the bottom left

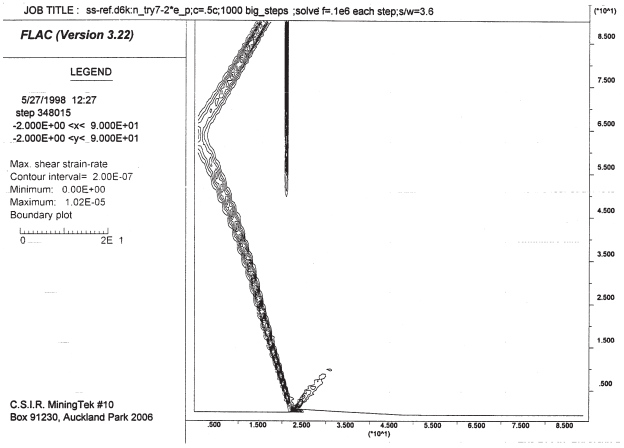

Figure 11—Contours of shear strain rate at ultimate load. A 90 by 90 m window is shown, with the 24 m wide half pillar at the bottom left

Theoretical background of the bearing capacity of a strip footing

The bearing capacity of foundations has been assessed from a theoretical viewpoint. Prandtl's original theoretical solutions (1920) and assumptions for the bearing capacity of a half mass under a strip load in two dimensions have been examined. Prandtl assumed an homogenous elastic-perfectly plastic material. Defining

$$S = \sin\phi \qquad [1]$$

where ϕ = friction angle, then the uniaxial compressive strength is:

$$UCS = 2c\sqrt{(1+S)/(1\pm S)} \qquad [2]$$

where c = cohesion,
then Prandtl's solution may be written as follows:

$$C = \frac{UCS}{2S}\left[(1+S)e^{\pi\tan(\phi)} - (1-S)\right] \qquad [3]$$

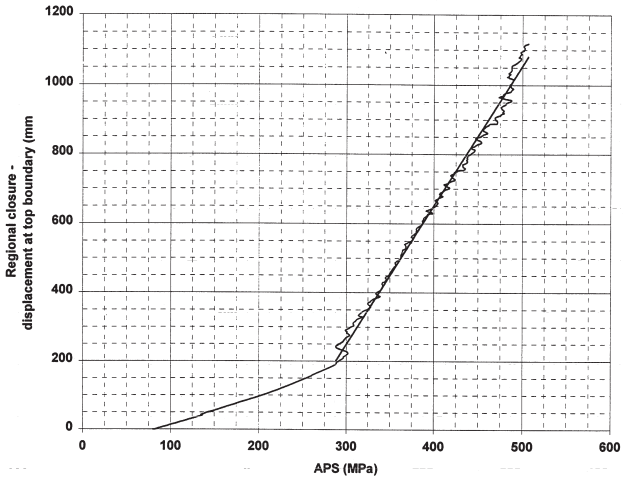

Figure 12—The displacement at the top boundary of the model (regional closure) as a function of the APS

where C is the Prandtl ultimate bearing capacity.

A graphical representation is given in Figure 13. From the equations above, it can be seen that the bearing capacity is a function of both the friction angle and the cohesion of the material. The solution implicitly assumes associated plasticity, that is, the dilation angle is equal to the friction angle. While rocks exhibit dilation, experimental evidence suggests that the dilation angle is less than the friction angle. This results in what is termed non-associated plasticity. Typical values for the friction angle lie between 30° and 50° for hard rocks, while typical values for the dilation angle for hard rocks are about 10°.

The effect of the reduced dilation angle on the bearing capacity on an approximate half plane was numerically modelled using FLAC (Figure 14). The friction angle was 40°, while the dilation angle was varied from 40° to 0°. A nominal value of cohesion, 100 kPa, was applied. Not only is the ultimate bearing capacity affected, but also the stiffness of the system. This effect was also noted by Vermeer and de Borst (1984). There is also a more pronounced change in slope at the yield point as the dilation angle decreases.

When the dilation angle was set equal to the friction angle, the FLAC model matched the velocity field predicted by Prandtl well. The surface area affected by heave, as a result of foundation failure, was also well predicted. Another effect of the non-associated dilation angle is that heave of the material adjacent to the foundation is greatly reduced. Rather, the 'Prandtl' wedge drives into the foundation, with a relatively small amount of heave predicted. Tensile failure adjacent to the edge of the pillar would also reduce the large-scale heave, and lead to local instability.

The same numerical analysis was performed for Witwatersrand quartzite. The properties are shown in Table II. The analytic bearing capacity, (Equation [3]) is C = 10 911 MPa, (with the dilation angle equal to the friction angle = 51°). When the dilation angle was set equal to the friction angle, the FLAC results matched the theoretical solution well. A reduction in the dilation angle to a more realistic value (10°), resulted in an ultimate bearing capacity of 5300 MPa, a reduction of over 50 per cent.

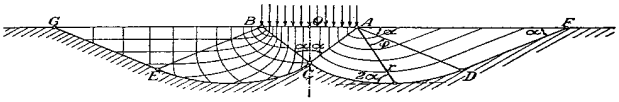

Figure 13—Wedge failure predicted by Prandtl (1920)

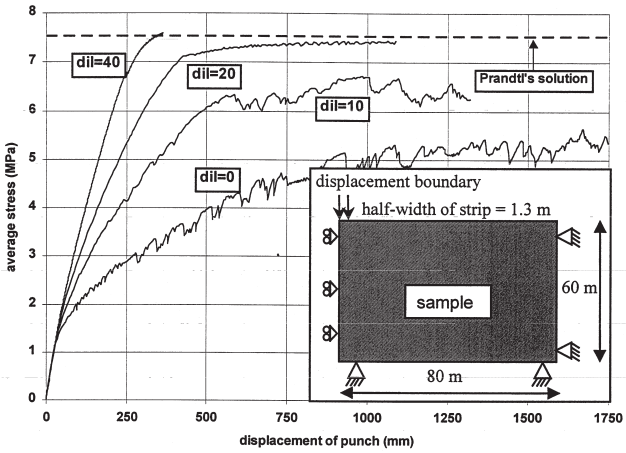

Figure 14—The effect of dilation angle on the bearing capacity of a strip footing. The friction angle was 40°, while cohesion was 100 kPa. The FLAC model to approximate an infinite half plane is shown

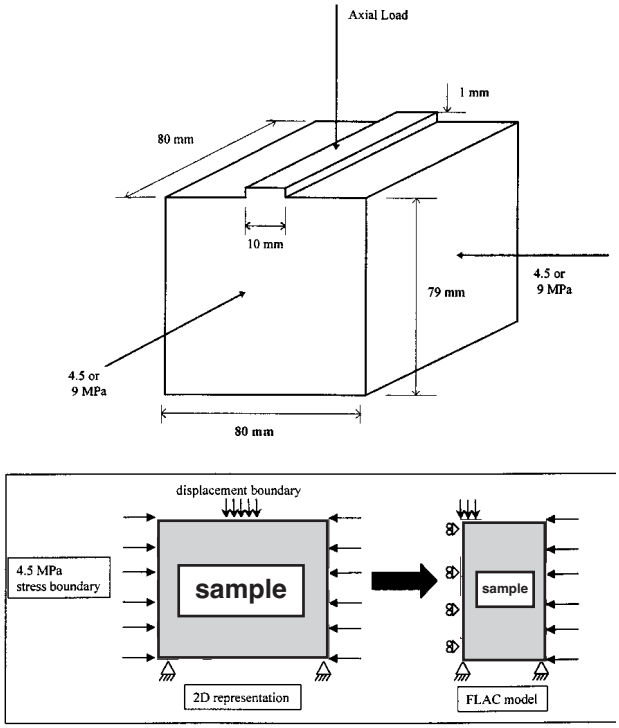

Figure 15—Geometry of the physical modelling of a strip pillar (after Dede, 1996). The equivalent FLAC model is shown below

A review of physical and numerical models of bearing capacity

Physical laboratory modelling of the bearing capacity of the foundation of a stabilizing pillar results in strengths considerably lower than that predicted by Prandtl's theory. There are a number of reasons for this. Firstly, Prandtl's theoretical solutions assume the dilation angle to be equal to the friction angle. For hard rock, the dilation angle is typically anything between a third and a fifth of the friction angle. The effect of this has been shown in the previous section. Secondly, the boundary conditions applied in laboratory modelling of foundation failure lead to weakening of the foundation. Thirdly, there are other factors, the influences of which are less easy to quantify. These include the effect of the brittleness of hard rock (assumed, in this paper, to be represented by a loss of cohesion as a function of plastic shear strain), and the micro-fracturing mechanics.

The second reason stated for the reduced laboratory strengths was the effects of the boundary conditions. Dede (1996) performed physical tests on 80 mm cubes of Witwatersrand quartzite (with material properties as shown in Table II). A 1 mm high, 10 mm wide strip 'pillar' was left intact in sample preparation (Figure 15). While the aim of the physical tests was not to model stabilizing pillar foundation failure *per se*, some observations are worthwhile. A confining pressure (4.5 or 9 MPa) was applied to the sides of the sample, while the sides were free to move in a vertical direction. This effectively created a geometry similar to Figure 2. The pressure boundary allowed the modelled plane of symmetry to dilate. This boundary, therefore, does not act as a true plane of symmetry. The effective confinement in the foundation is, therefore, reduced. A numerical simulation of the physical model was performed using the material parameters shown in Table II. The model geometry is also shown in Figure 15. The ultimate bearing capacity was about 650 MPa, which agreed well with the physical test results. This was about 2.5 times the UCS of the material and, coincidentally, agrees with the guidelines mentioned earlier (Anon, 1988).

In a deep level gold mine repeating pillar layout, the effective vertical planes of symmetry along the centre lines of the panels lead to a much stiffer system. This is especially true of SMDP mining. A true repeating geometry was numerically modelled using vertical planes of symmetry along the stope and pillar centre lines. The geometry of the model was exactly the same as the numerical model of Dede's laboratory tests, except that the stress boundary on the right-hand side (Figure 15) was replaced by a vertical plane of symmetry. The more rigid system results in an increase in the ultimate bearing capacity to about 8000 MPa, with Mohr-Coulomb material. Thus, the rigid boundary conditions have led to about a twelve-fold increase in the bearing capacity. The horizontal stresses at the right-hand boundary of the

Table II

Material parameters of quartzite used in numerical modelling of Prandtl's wedge (after Dede, 1996)

Material Property	Value
Shear Modulus	29.1 GPa
Bulk Modulus	34.3 GPa
Density	2700 kg/m^3
Cohesion	35 MPa
Friction angle	51°
Dilation angle	51° or 10°

model, some way beneath the surface, were over 900 MPa at the ultimate stress level. By comparison, the stresses at the equivalent location in the model of the semi-infinite half plane (Figure 14) were about 250 MPa.

Rock in deep level gold mines exhibits brittle behaviour, which may be expressed as cohesion loss as a function of plastic shear strain. A series of FLAC strain hardening/softening models were run at various rates of cohesion softening for the rigid boundary model (repeating pillar geometry). The cohesion was reduced linearly from 35 MPa to 0.5 MPa as a function of plastic shear strain. The plastic shear strain at which cohesion was set to 0.5 MPa varied from 5 to 20 mε (i.e. the *strain rate* was varied). The ultimate bearing capacity was affected, ranging from 2000 to 2500 MPa. The post yield modulus was also affected. However, the yield point for the Mohr-Coulomb and all the strain hardening/softening models was the same, as shown in Figure 16. Note that the yield point for the rigid boundary and the 9 MPa boundary is shown to be the same. However, the post yield modulus is markedly different.

Wagner and Schümann (1971) performed punch tests on five rock types. The rock samples were 150 mm in diameter and 100 mm long. The samples were encased in steel jackets. The initial confinement provided to the samples was nominal, to prevent tensile splitting of the samples (Wagner, 1997). The results of the tests on quartzite are shown in Table III. The trend of decreasing capacity with increasing ratio of punch to sample dimension is clear.

Cook *et al.* (1984), performed punch tests on cylindrical specimens of granite, encased in steel cylinders. The rock samples were 89 mm in diameter and length. The steel was heat shrunk onto the specimens to provide a confining stress of 27 MPa to the rock. When the punch was 5 mm in diameter (about 1/20th of the diameter of the rock sample), the bearing capacity was about 12 times the UCS of the material. When the punch was 20 mm in diameter (1/5th of the diameter of the rock sample), the bearing capacity was just under 10 times the UCS of the material (see Figure 17).

The tests of Cook *et al.* (1984) have been back analysed using FLAC. The results of the Mohr-Coulomb constitutive model overestimated the strength. Strain hardening/softening models provided fairly good results. In all cases however, the yield point of the foundation was the same, whether for the Mohr-Coulomb material, or for various rates of plastic strain softening (10 to 20 mε).

Discussion and proposed new design consideration for the bearing capacity of stabilizing pillar foundations

The boundary conditions applied in the physical modelling performed by Dede (1996) have been shown to have a direct influence on the ultimate bearing capacity of the samples. Numerical modelling has shown that the change from a 9 MPa stress boundary to a rigid boundary results in a twelve-fold increase in bearing capacity for a Mohr-Coulomb material.

In comparing the results of the physical tests performed by Cook *et al.* (1984) and Wagner and Schümann (1971), it is postulated that the difference lies in the confining pressure provided by the steel cylinder in the tests performed by Cook

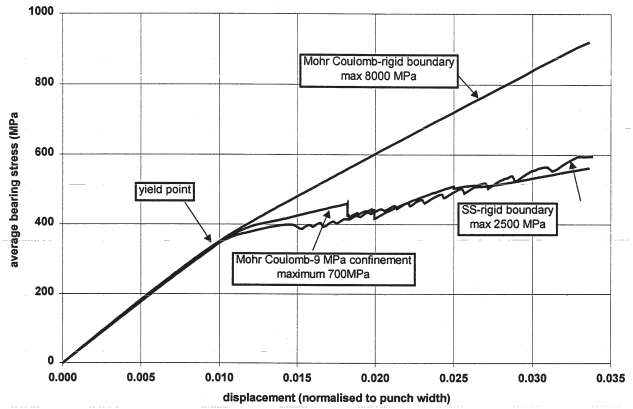

Figure 16—The numerically modelled yield points for various boundary conditions and material models of the foundation of a strip pillar

Table III

Bearing capacity of quartzite rock sample with different steel punch sizes (after Wagner and Schümann (1971)

Punch diameter (mm)	Punch diameter ÷ sample diameter	Bearing capacity ÷ UCS
3.81	0.0254	13
7.62	0.0508	10
15.24	0.1016	7
30.48	0.2032	5

et al. Cook *et al* applied an interference fit of the steel cylinder such that, given the dimensions and properties of the rock and steel, the radial stiffness of a semi-infinite half mass was approximated to within 10 per cent. The confining pressure was 27 MPa. Thus, the difference between the punches at approximately 1/20th and 1/5th of the diameter of the rock sample led to a relatively small difference in bearing capacity (Figure 17). By contrast, the difference in bearing capacity, as the punch diameter is increased, is much more marked in the results reported by Wagner and Schümann (1971). As the ratio of punch to sample diameter gets larger, the effect of the boundary becomes more important, which explains the difference in trend between the two curves shown in Figure 17.

Physical modelling of foundation load bearing capacity has been shown to be strongly influenced by the boundary conditions. It is suggested that the boundary conditions of repeating *in situ* stabilizing pillars are not adequately represented by any physical tests performed thus far. It is suggested that the true ultimate bearing capacities of foundations have not yet been determined, and are larger than has been supposed thus far. The numerical modelling shows that the stress levels associated with deep level gold mines are within the ultimate bearing capacity of the foundations.

Handley *et al.* (1997) found that pillar associated seismicity initiated in the back areas at WDL when the APS

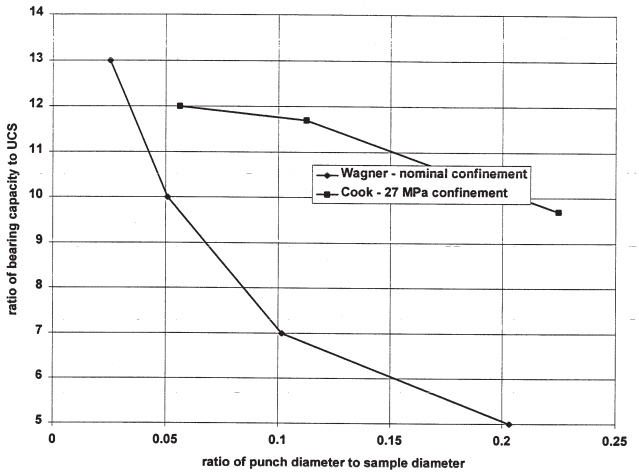

Figure 17— A comparison of the effects of punch diameter, normalized to sample diameter, on the bearing capacity, normalized to the UCS of the material, of samples with and without confining pressure

was, on average, 1.2 times the UCS of the footwall rock. Lenhardt and Hagan (1990) found that pillar foundation associated seismicity occurred in the range 65-95 m from the face. In both of these cases, the APS was not the full load that the pillar would receive. It is suggested that these histories of 'foundation failure' are, rather, symptoms of the yielding of the pillar/foundation system.

This is supported by the numerical modelling (Figure 5), in which it can be seen that the pillar/foundation system continues to accept load, despite the yielding of the system at about 57 per cent of the final load (the final load corresponds to the depth and extraction ratio). Associated with this, is the occurrence of a characteristic 'Prandtl' wedge, along with a sub plane of failure, perpendicular to the reef plane (Figure 7 and Figure 11). The regional load-deformation characteristics of the system also change (see Figure 12). The system becomes 'softer'. The yield point on the load-displacement curve of the foundation (Figure 12) is associated with stress levels currently encountered in the foundations of stabilizing pillars in deep level gold mines.

Taking all the above arguments into account, and if one of the aims of mine planning is to reduce pillar/foundation system seismicity, then the point of interest for design purposes lies in the yield point of the foundation. A reduction in pillar/foundation system seismicity implies a reduction in regional closure. This implies a reduction in regional ERR (Özbay and Ryder, 1990).

Previously, the design criterion for the stability of the foundation has stipulated that the average pillar stress (APS) must be less than 2.5 times the UCS of the foundation material. However, the UCS of a material is a function of both the cohesion and friction angle (see Equation [2]). Different materials of the same UCS may have different combinations of cohesion and friction angle. The design criterion mentioned takes into account only superficially the strengthening effect of confinement. It is proposed, therefore, that the yield point, and hence the criterion, be determined in terms of cohesion and friction angle, as well as the effective confining pressure, as separate variables.

Some preliminary modelling has been performed, to determine the effects of cohesion, and the interaction between friction angle and confining pressure. A repeating pillar geometry was modelled in FLAC. For these preliminary results, the effects of gradual pillar loading as a result of the removal of the stope, were not modelled. The foundation was loaded by means of a displacement boundary. The values of friction angle were 30°, 51° and 54°, and the values of cohesion were 25, 35 and 65 MPa. An increase in confining pressure may be regarded, crudely, for the purposes of a preliminary design nomogram, as correlating with increasing depth.

The results are presented in the form of a preliminary design nomogram (Figure 18). The three design variables are: cohesion and friction angle of the foundation material, and the horizontal stress (and thereby the effective mining depth, having assumed a *k* ratio). The circled points on the nomogram correspond to FLAC runs performed to construct the nomogram. To determine the yield point of a foundation at a depth of 2222 m (corresponding to σ_h = 30 MPa, *k* ratio = 0.5, rock density = 2700 kg/m^3), with the foundation cohesion and friction angle 35 MPa and 51° respectively, one may follow the sequence A to D as indicated in Figure 18.

Özbay and Ryder (1989) performed physical tests that were similar in terms of geometry and boundary conditions to the numerical modelling used to construct the nomogram. The load-displacement curves for their tests on quartzite, as well as the physical model geometry, are shown in Figure 19. Özbay and Ryder reported that the average peak APS was 675 MPa for the five tests. Using the solid horizontal line drawn on the load-displacement curve in Figure 19, the average of the peak loads is estimated to be 11.0 MN. The confining stress supplied in the tests was 40 MPa, while the cohesion and friction angle were 65 MPa and 54° respectively. Using the design nomogram in Figure 18, the predicted value of the yield point is 490 MPa. The corresponding load for an APS of 490 MPa is: (490/675) x 11 = 8.0 MN. This is marked with the dashed line in Figure 19. As may be seen, the agreement with the actual yield points is good.

The use of backfill would result in an increase in the effective horizontal stress in the foundation. According to the new design considerations, an increased yield strength would be predicted. Hagan (1998) notes that the use of backfill with strike stabilizing pillars at WDL East Mine has resulted in increased stability. The broken lines in Figure 18 show, conceptually, the effect of backfill for ϕ = 30° and 54°.

The friction angle and cohesion may be determined from laboratory testing as follows. A suitable testing program would include UCS tests, and triaxial tests at a range confining pressures, for example 10, 20 and 40 MPa. The peak strengths of the tests may be plotted on a graph with the peak stresses as a function of confining pressure (as in Figure 3). For hard rocks, a linear function usually describes the relation well. If such a linear function is defined as:

$$\sigma_1 = \beta\sigma_3 + \overline{UCS} \qquad [4]$$

where σ_1 = peak strength and
σ_3 = confining pressure,
then the cohesion (*c*) is written as:

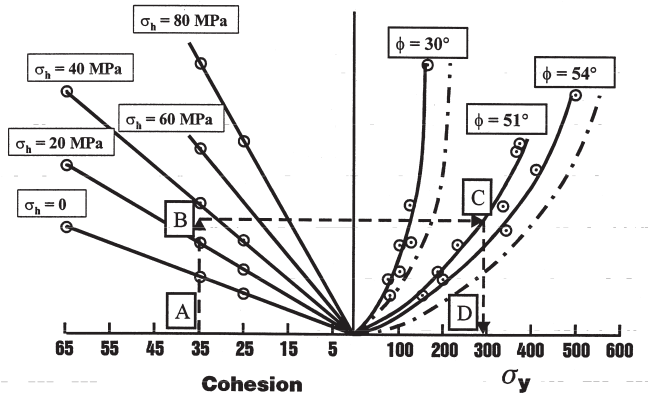

Figure 18—A preliminary design nomogram to determine the yield point of stabilizing pillar foundations. The effect of backfill is shown conceptually with the broken lines for ϕ = 30° and ϕ = 54°

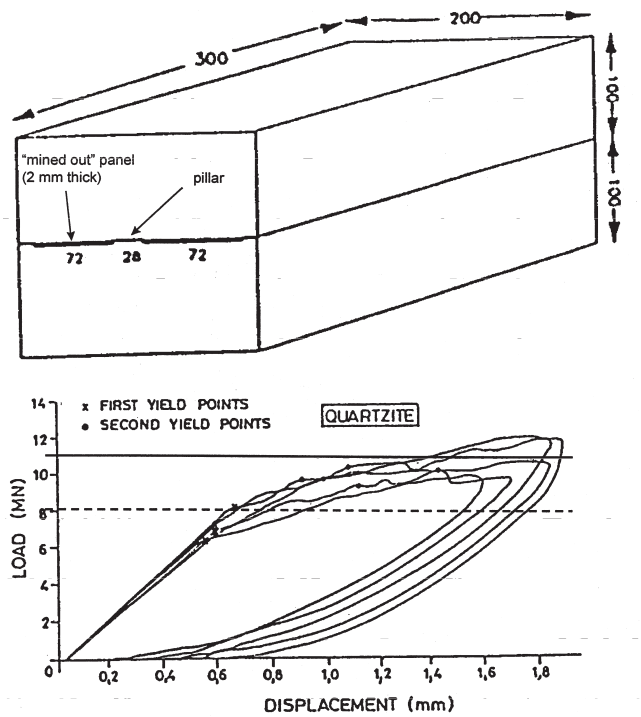

Figure 19—Geometry and results of physical modelling on quartzite (after Özbay and Ryder, 1989). The yield point predicted by the use of the nomogram in Figure 18, is shown by the dashed line

$$c = \frac{\overline{UCS}}{2\sqrt{\beta}} \qquad [5]$$

and the friction angle (ϕ) is written as:

$$\phi = \sin^{-1}\left(\frac{\beta - 1}{\beta + 1}\right). \qquad [6]$$

Conclusions

In situ 'foundation failure' is probably best viewed as the onset of the first significant yielding of the foundation, rather than the ultimate bearing capacity of the foundation. The foundation continues to accept load after yielding. For foundations that consist of brittle rock, it is postulated that *in situ* stabilizing pillar foundation associated seismicity, such as has been measured at WDL, is associated with this yielding phenomenon. The yielding of foundations in a more plastic rock would be associated with a significant increase in the closure rate (i.e. 'footwall heave'). The numerical modelling shows that there is very considerable capacity after the yield point. The *ultimate* bearing capacity of the foundations of stabilizing pillars is not yet known. Numerical modelling alone should not be relied upon to determine this value, due to the unknowns inherent in the post yield process. There is a need for the design of suitable laboratory experiments to determine the ultimate bearing capacity.

A new design methodology is proposed to enable the yield point of the foundation of deep level stabilizing pillars to be predicted in terms of the cohesion, friction angle and depth. The friction angle accounts for different confining stresses with depth, and would also account for the additional confining effects of backfill.

The technical advantages of this approach are as follows:

- the effect of different cohesion and friction angles may be taken into account, even though the materials may have the same UCS
- the confining effect of the horizontal stresses at greater depths may be taken into account
- the effect of backfill may be included in designer.

These advantages will enable mine layout designers to predict pillar/foundation system associated seismicity. Although it may not be possible to prevent foundation yielding altogether, the prediction of such yielding would provide the opportunity to plan extraction and excavations to minimize potential damage as a result of seismicity associated with foundation yielding. These technical benefits would lead to production and safety benefits as a result of better mine planning.

To prevent significant increases in ERR associated with the yielding of the pillar/foundation system, the extraction ratio must be such that the yield points are not significantly exceeded. Alternatively, the yield point may be increased by increasing the effective confining pressure in the foundation by the use of backfill. The use of the proposed design nomograms may allow for a combination of these measures in the design process.

There are a number of unknowns with respect to the yielding of pillar/foundation systems. Some are:

- the detailed mechanisms of yielding as a function of load
- it is suspected that the mechanism of yielding changes with time
- the deformation of the pillar and surrounding rock mass
- the effect of the strata dip angle (not relevant for SMDP).

An *in situ* monitoring program, together with additional numerical modelling, would be required to establish these fundamentals, and therefore to also adjust and calibrate the preliminary design nomogram. The effects of the *in situ* stress tensor, and the path dependency of load transfer onto the pillar as a result of removing the stope should also be

investigated, both numerically and by *in situ* monitoring.

It should be noted that any design consideration based on plane strain analysis would neglect the effect of geological structures in the plane. The effects of such structures would have to be individually modelled and monitored.

Acknowledgements

Part of this work was carried out under SIMRAC project GAP 223. Funding for this research is gratefully acknowledged. Special thanks are due to the management of Kloof Gold Mine for allowing research activities to be conducted at underground sites.

References

ANON. Industry guide to the amelioration of the hazards of rockbursts and rockfalls. Johannesburg, *Chamber of Mines of South Africa Research Organization*, 1977.

ANON. An industry guide to methods of ameliorating the hazards of rockfalls and rockbursts. Johannesburg, *Chamber of Mines of South Africa Research Organization*, 1988.

COOK, N.G.W., HOOD, M., and TSAI, F. Observations of crack growth in hard rock loaded by an indenter. *Int. J. Rock Mech. & Geomech*. Abstr. Vol. 21, no. 2. 1984. pp. 97–107.

DEDE, T. Investigations into the mechanism of fracture onset and growth in layered rock using physical and numerical modelling. M.Sc. dissertation, University of the Witwatersrand, 1996.

HAGAN, Pers. comm., 1988.

HANDLEY, M.F., SELFE, D.A., VIEIRA, F.M.C.C., MACCELARI, M.J. and DEDE, T. Current position of strike stabilizing and bracket pillar design—Guidelines for deep level tabular orebodies. *J. S. Afr. Inst. Min. Metall.*, vol. 97, no. 3. May/June, 1997. pp. 103–117.

KERSTEN, R.W.O. and LEACH, A.R. The calibration of material models in FLAC for deep level gold mines. *Eurock '96*. ISRM International Symp., Torino, Balkema, 1996.

LEACH, A.R., and LENHARDT, W.A. Pillar associated seismicity at Western Deep Levels Mine. *Static and Dynamic considerations in Rock Engineering*. Brummer (ed.), Balkema, Rotterdam, 1990.

LENHARDT, W.A. Seismicity associated with deep-level mining at Western Deep Levels Limited. *J. S. Afr. Inst. Min. Metall.*, vol. 92, no. 5. May, 1992. pp. 113–120.

LENHARDT, W.A. and HAGAN, T.O. Observations and possible mechanisms of pillar-associated seismicity at great depth. *Technical Challenges in Deep Level Mining*. Johannesburg, SAIMM, 1990.

ÖZBAY, M.U. and RYDER, J.A. Investigations into foundation failure mechanisms of hard rock squat pillars. *Rock at Great Depth*, ISRM Symp., Pau, 1989, Balkema, 1989.

ÖZBAY, M.U. and RYDER, J.A. The effects of foundation damage on the performance of stabilizing pillars. *J. S. Afr. Inst. Min. Metall.*, vol. 90, no. 2. Feb. 1990. pp. 29–35.

PRANDTL, L. Über die Eindringungsfestigkeit (Härte) plastischer Baustoffe und die Festigkeit con Schneiden Z. Agnew Matt. Mech. Vol. 1, 1920. pp. 15–20.

RYDER, J.A. Personal communication, 1994.

RYDER, J.A. Personal communication, 1997.

SALAMON, M.D.G. Two-dimensional treatment of problems arising from mining of tabular deposits in isotropic or transversely isotropic ground. *Int. J. Rock Mech. & Geomech*. Abstr. Vol. 5, 1963. pp. 159–185.

VERMEER, P.A. and DE BORST, R. Non-associated plasticity for soils, concrete and rock. Heron, vol. 29, no. 3. 1984. pp. 1–64.

VIEIRA, F.M.C.C. Review of criteria for stabilizing pillar design. *1st Southern African Rock Engineering Symposium*, Johannesburg, South Africa, 1997. pp. 210–227.

VLIETSTRA, D. *In situ* stress measurements at Kloof Gold Mine using the 'doorstopper' technique. Internal Note RE 1/95, CSIR, Division of Mining Technology, 1995.

WAGNER, H. Pers. comm. 1997.

WAGNER, H. and SCHÜMANN, E.H.R. The stamp-load bearing strength of rock—An experimental and theoretical investigation. *Rock Mechanics*, vol. 3, 1971. pp. 185–207.

YORK, G. The rock mechanics viability of replacing rock stabilizing pillars in deep level gold mines with concrete. M.Sc. dissertation, University of the Witwatersrand, 1997.

Appendix

Data file and user defined (FISH) files for model to simulate total closure

```
*** SS-REF.D6M
*** call fixwh_st.fis-does tot_clos_chk as a WHILE_STEPPING
function
*** do whole run under RELAX, n_big_steps 1000
*** remove n_small_steps : do SOLVE force .1e6 for each
n_big_step
*** n-try7 para's, but 2*e_p
*** apply sxx=0=syy to pillar side wall
*** c=1/2c
***
***
set log ssrefd6m.log
new
title
ss-ref.d6m:n_try7-2*e_p;c=.5c;1000 big_steps;solve f=.1e6
each step;tot_clos
conf extra 4
grid 130 266
model ss
*
set large
*
prop d 2700 sh 28.8e9 bu 41.8e9
prop coh 25.4e6 fric 21.6 dil 0 tens 18e6
*
prop ctab=1
table 1 0,25.4e6 .001,25.4e6 .002,22.6e6 .008,5.4e6
.009,3.4e6 .01,1.8e6
table 1 .011,0.8e6 .012,.4e6
prop ftab=2
table 2 0,21.6 .001,34 .002,37.6 .003,40 .004,41.6 .005,42.4
prop dtab=3
table 3 0,0 .004,10 .02 0
*
gen 0,0 0,0.6 24,0.6 24,0  i=1,33  j=1,3   rat 0.949445 1    ;
Area 1
gen same 0,100 24,100 same i=1,33  j=3,137  rat 0.949445
1.012167 ; Area 2
gen same 0,320 24,320 same i=1,33  j=137,267 rat
0.949445 1    ; Area 3
gen same same 48,0.6 48,0  i=33,65 j=1,3   rat 1.053247 1
; Area 4
gen same same 48,100 same  i=33,65 j=3,137  rat 1.053247
1.012167 ; Area 5
gen same same 48,320 same  i=33,65 j=137,267 rat
1.053247 1    ; Area 6
gen same same 160,0.6 160,0 i=65,131 j=1,3          ; Area 7
gen same same 160,100 same i=65,131 j=3,137  rat 1
1.012167 ; Area 8
gen same same 160,320 same i=65,131 j=137,267          ;
Area 9
*
ini sxx=-40e6 syy=-80e6 szz=-40e6
```

```
fix x i=1
fix x i=131
fix y j=1
apply syy=-80e6 j=267
*
hi nst=50
hist unbal
*
hist syy i=1 j=1
hist syy i=5 j=1
hist syy i=10 j=1
hist syy i=15 j=1
hist syy i=18 j=1
hist syy i=21 j=1
hist syy i=24 j=1
hist syy i=27 j=1
hist syy i=28 j=1
hist syy i=29 j=1
hist syy i=30 j=1
hist syy i=31 j=1
hist syy i=32 j=1
*
hist syy i=27 j=2
hist syy i=28 j=2
hist syy i=29 j=2
hist syy i=30 j=2
hist syy i=31 j=2
hist syy i=32 j=2
*
hist ydis i=28 j=3
hist ydis i=29 j=3
hist ydis i=31 j=3
hist ydis i=32 j=3
hist ydis i=34 j=3
hist ydis i=48 j=3
hist ydis i=65 j=3
hist ydis i=100 j=3
hist ydis i=131 j=3
*
ca pill-aps.fis
set pill_edge = 32
hist flac_y_strss1
*
* ca fixwh_st.fis
* while_stepping-checks for ydis <= -.6; fixes g.p. in yvel=0
* keep track of whether grid point has been fixed(ex_3) and
at what step(ex_4)
* i1,i2,j2 same as in zonk.fis (ZONK and RELAX must all
ready have run)
ca fixwh_st.fis
*
* found-f8.fis - while_stepping
* monitors for failure under pillar centre line in stabilising
pillars
* run automatically during RELAX in ss-ref.d6m (whole run
under RELAX)
* sets fail2 = 1 the first time ff is detected
* RELAX in zonkd6m.fis checks for fail2 = 1 ==> does sav
file
*
ca found-f8.fis
ca top_clos.fis ; monitors avg closure at top of model
set height = 320
hi top_clos
hi top_strn
ca pillstrn.fis ; avg axial strain of pillar
set stope_width=0.6
hi pillstrn
ca stp-strs.fis
*
* ca zonkd6m.fis
* RELAX factor is taken to be uniform again
* modify to SOLVE FORCE=.1E6 at each big step (instead of
n_small_steps)
* do sav files according to no. of big_steps given in table 4
* do tmp sav file after each big_step
* remove sxx, syy forces at pillar side wall-creates false
confinement
*
table 4 1,250 2,500 3,625 4,750 5,875 6,1000
ca zonkd6m.fis
set n_big_steps 1000
set i1 33 i2 130 j1 1 j2 2
total_stope
hist total_stope
hist left_stope
hist right_stope
zonk
relax
```

```
* PILL-APS.FIS
* calculate APS of pillar in quarter symmetery; pillar in
bottom left corner
* input : pill_edge = no. of zones in pillar
* pill_edge may vary as zones at pillar edge are nulled
def flac_y_strss1
  total_area=0
  total_force=0
  loop i (1,pill_edge)
   ar = x(i+1,1) - x(i,1)
   total_area = total_area + ar
   force = syy(i,1) * ar
   total_force = total_force + force
  end_loop
  flac_y_strss1 = total_force / total_area
end
*
def flac_y_strss2
  total_area=0
  total_force=0
  loop i (1,pill_edge)
   ar = x(i+1,3) - x(i,3)
   total_area = total_area + ar
   force = syy(i,3) * ar
   total_force = total_force + force
  end_loop
  flac_y_strss2 = total_force / total_area
end
```

```
; FIXWH_ST.FIS
; while_stepping-checks for ydis <= -.6; fixes g.p. in yvel=0
;
; keep track of whether grid point has been fixed(ex_3) and
```

```
at what step(ex_4)
; i1,i2,j2 same as in zonk.fis (ZONK and RELAX must
allready have run)
; stope width must be checked for each model
def tot_clos_chk
 while_stepping
 int no_of_fixes
 i2p1=i2+1
 j2p1=j2+1
 loop i (i1,i2)
  ip1=i+1
  if ex_3(ip1,j2p1) = 0 then
   if ydisp(ip1,j2p1) <= -0.6 then ;check that 0.6 is correct
stope width
    yvel(ip1,j2p1) = 0
    flags(ip1,j2p1) = or(flags(ip1,j2p1),4)
    ex_3(ip1,j2p1) = 1
    ex_4(ip1,j2p1) = step
    no_of_fixes=no_of_fixes+1
   end_if
  end_if
 end_loop
end
```

```
* FOUND-F8.FIS
* while_stepping
* monitors for failure under pillar centre line in stabilising
pillars
* run automatically during RELAX in ss-ref.d6m (whole run
under RELAX)
* sets fail2 = 1 the first time ff is detected
* RELAX in zonkd6m.fis checks for fail2 = 1 ==> does sav
file
def found_fail
  while_stepping
  int fail1 fail2
  loop j (j2+1,200)
   case_of state(1,j)
    case 1
     fail1=1
    case 2
     fail1=1
    case 10
     fail1=0 ; to ensure max state value does not bomb
program
   end_case
  end_loop
  if fail2 = 0 then
   if fail1 = 1 then
    fail2 = 1
   end_if
  end_if
end
```

```
* TOP_CLOS.FIS
* finds average closure for top of model - used in \reef\elas-
ref.d2b
* finds average strain over whole height
* must supply height of model
def top_clos
 vol=0
 loop i (1,izones)
  vol = vol + 0.5*(x(i+1,jgp)-
x(i,jgp))*(ydisp(i,jgp)+ydisp(i+1,jgp))
 end_loop
 top_clos = vol / (x(igp,jgp) - x(1,jgp))
 top_strn = vol / (x(igp,jgp) - x(1,jgp)) / height
end
```

```
* PILLSTRN.FIS
* calculate avg strain of pillar - used in \reef\elas-ref.d2b
*
def pillstrn
 int stope_width pill_edge
 vol=0
 loop i (1,pill_edge)
  vol = vol + 0.5*(x(i+1,j2p1)-
x(i,j2p1))*(ydisp(i,j2p1)+ydisp(i+1,j2p1))
 end_loop
 pillstrn = vol / (x(pill_edge,j2p1) - x(1,j2p1)) / stope_width
end
```

```
; STP-STRS.FIS
; monitor stress build up in stope-produce average stress
; do whole stope start from pillar edge (pillar bottom left
corner)
; assuming full closure is indicated in ex_3 (1=compl.
closure, 0=non-c.c.)
def total_stope
 j2p1 = j2 + 1 ; j2 known from RELAX.FIS
 width = 0
 load = 0
 end_flag = 0 ; =1 —> end of pillar adjacent closure
 left_flag = 0 ; =1 —> pillar adjacent stress has allready been
calculated
 clos_flag=0 ; =1 —> complete stope closure has been
detected
 loop icount(i1,i2) ; i1 and i2 known from RELAX.FIS
  if ex_3(icount,j2p1) = 1 then
   ip1 = icount + 1
   if ex_3(ip1,j2p1) = 1 then ;check next grid point has
closed
     width = width + (x(ip1,j2p1) - x(icount,j2p1))
     load = load + syy(icount,j2p1)*(x(ip1,j2p1) -
x(icount,j2p1))
              clos_flag=1
              end_flag=0
   else
     end_flag = 1
   end_if
  end_if
  if end_flag = 1 then
   if clos_flag = 1 then
    if left_flag = 0 then
              left_flag = 1
              left_stope = load / width
              left_load = load
              left_width = width
             end_if
            end_if
  end_if
 end_loop
```

```
 if clos_flag = 1 then
   total_stope = load / width
   right_load = load - left_load
   right_width = width - left_width
   if right_width > 0.0 then ; may only have closed adjacent to
pillar
    right_stope = right_load / right_width
   end_if
 end_if
end
```

```
* ZONKD6M.FIS
* zonk and relax functions for ss-ref.d6m
* pillar_factor is linear
* while_stepping tot_clos_chk checks for total closure
* modify to SOLVE FORCE=.1E6 at each big step (instead of
n_small_steps)
* remove side wall forces-creates false confinement
* do sav files according to no. of big_steps given in table 4
* do tmp sav file after each big_step
* check for fail2 = 0 from found-f8.fis ==> ff
* do a minimum of 10 steps (in case unbal force is below
.1e6)
def zonk
;
; Extract given region of zones and store existing forces on
; the boundary of this region in extra arrays 6 and 7.
; INPUT: i1, i2 bounding i-numbers of region (i2 > i1)
;     j1, j2 bounding j-numbers of region (j2 > j1)
;
 j2p1 = j2 + 1
 i2p1 = i2 + 1
 loop i (i1,i2p1) ; (record existing fix conditions)
  loop j (j1,j2p1)
   ex_1(i,j) = 0.0
   ex_2(i,j) = 0.0
   if and(flags(i,j),2) # 0 then
    ex_1(i,j) = 1.0
   end_if
   if and(flags(i,j),4) # 0 then
    ex_2(i,j) = 1.0
   end_if
  end_loop
 end_loop
 command ; (allow forces to act on boundary grid-points)
  model null i=i1,i2 j=j1,j2
  fix x y i=i1,i2p1 j=j1,j2p1
  ini xv=0 yv=0 i=i1,i2p1 j=j1,j2p1
  step 1
  free x y i=i1,i2p1 j=j1,j2p1
 end_command
 loop i (i1,i2p1) ; (restore fix conditions)
  loop j (j1,j2p1)
   if ex_1(i,j) # 0.0 then
    flags(i,j) = or(flags(i,j),2)
   end_if
   if ex_2(i,j) # 0.0 then
    flags(i,j) = or(flags(i,j),4)
   end_if
  end_loop
 end_loop
 loop ii (i1,i2p1)
  loop jj (j1,j2p1)
   if and(flags(ii,jj),8) = 0 then
    ex_1(ii,jj) = xforce(ii,jj)
    ex_2(ii,jj) = yforce(ii,jj)
    xfa = -xforce(ii,jj)
    yfa = -yforce(ii,jj)
    command
     apply xforce=xfa yforce=yfa i=ii j=jj
    end_command
   end_if
  end_loop
 end_loop
end

def relax
;
; Relax forces around newly-mined region gradually.
; INPUT: n_big_steps  = number of reductions in applied
forces
;     n_small_steps = number of FLAC steps within each of the
above
;              steps
; modify to SOLVE FORCE=.1E6 at each big step
; do a minimum of 10 steps (in case unbal force is below
.1e6)
; do NOT use pillar_factor from table, uniform factor as before
int n_big_steps      prev_step no_of_steps
 fail3=0 ; ensures only save ff file once
 loop n (1,n_big_steps)
  prev_step = step
  top  = 1.0 * (n_big_steps - n)
  bot  = 1.0 * n_big_steps
  factor = top / bot
  command
   set echo off
  end_command
  loop i (i1,i2p1)
   loop j (j1,j2p1)
    if and(flags(i,j),8) = 0 then
     xfa = -ex_1(i,j) * factor
     yfa = -ex_2(i,j) * factor
     command
      apply xforce=xfa yforce=yfa i=i j=j
     end_command
    end_if
   end_loop
  end_loop
  loop j (j1,j2p1)
   command
    apply xforce=0 yforce=0 i=i1 j=j ;remove side wall forces
   end_command
  end_loop
  command
   set echo on
   print factor
   solve step=20000 force=.1e6
  end_command
  if step < prev_step + 10 then
   no_of_steps = 10 - (step-prev_step)
   command
```

```
   step no_of_steps
  end_command
 end_if
 command
  sav tmpd6m.sav
 end_command
 loop jj (1,6) ; intermediate save files
  if n = table(4,jj) then
   name = 'ssrefd6m.s0' + string(jj)
            command
             sav @name
            end_command
  end_if
 end_loop
 if fail3 = 0 then
  if fail2 = 1 then ; from found-f8 -signifies failure under
pillar centre line
   command
    sav ssrefd6m.sff ; sff = save @ failure under pillar centre
line
   end_command
            fail3 = 1
  end_if
 end_if
end_loop
end
```

Data file and fish files for non total closure model

```
*** SS-REF.D6K
*** n-try7 para's, but 2*e_p
*** avoid tot_clos
*** do whole run under RELAX, n_big_steps 1000
*** remove n_small_steps : do SOLVE force .1e6 for each
n_big_step
*** apply sxx=syy=0 to pillar side wall
*** c=1/2c
set log ssrefd6k.log
new
title
ss-ref.d6k:n_try7-2*e_p;c=.5c;1000 big_steps;solve f=.1e6
each step;s/w=3.6
conf extra 4
grid 130 270
model ss
*
set large
*
prop d 2700 sh 28.8e9 bu 41.8e9
prop coh 25.4e6 fric 21.6 dil 0 tens 18e6
*
prop ctab=1
table 1 0,25.8e6 .001,25.4e6 .002,22.6e6 .008,5.4e6
.009,3.4e6 .01,1.8e6
table 1 .011,0.8e6 .012,.4e6
prop ftab=2
table 2 0,21.6 .001,34 .002,37.6 .003,40 .004,41.6 .005,42.4
prop dtab=3
table 3 0,0 .004,10 .02 0
*
gen 0,0 0,1.8 24,1.8 24,0  i=1,33  j=1,7   rat 0.949445 1    ;
Area 1
gen same 0,100 24,100 same i=1,33  j=7,141  rat 0.949445
1.012167 ; Area 2
gen same 0,320 24,320 same i=1,33  j=141,271 rat
0.949445 1    ; Area 3
gen same same 48,0.6 48,0  i=33,65 j=1,7   rat 1.053247 1
; Area 4
gen same same 48,100 same  i=33,65 j=7,141  rat 1.053247
1.012167 ; Area 5
gen same same 48,320 same  i=33,65 j=141,271 rat
1.053247 1    ; Area 6
gen same same 160,0.6 160,0 i=65,131 j=1,7            ; Area 7
gen same same 160,100 same i=65,131 j=7,141  rat 1
1.012167 ; Area 8
gen same same 160,320 same i=65,131 j=141,271            ;
Area 9
*
ini sxx=-40e6 syy=-80e6 szz=-40e6
fix x i=1
fix x i=131
fix y j=1
apply syy=-80e6 j=271
*
hi nst=50
hist unbal
*
hist syy i=1 j=1
hist syy i=5 j=1
hist syy i=10 j=1
hist syy i=15 j=1
hist syy i=18 j=1
hist syy i=21 j=1
hist syy i=24 j=1
hist syy i=27 j=1
hist syy i=28 j=1
hist syy i=29 j=1
hist syy i=30 j=1
hist syy i=31 j=1
hist syy i=32 j=1
*
hist syy i=27 j=2
hist syy i=28 j=2
hist syy i=29 j=2
hist syy i=30 j=2
hist syy i=31 j=2
hist syy i=32 j=2
hist ydis i=28 j=7
hist ydis i=29 j=7
hist ydis i=31 j=7
hist ydis i=32 j=7
hist ydis i=34 j=7
hist ydis i=48 j=7
hist ydis i=65 j=7
hist ydis i=100 j=7
hist ydis i=131 j=7
*
ca pill-aps.fis
set pill_edge = 32
hist flac_y_strss1
* found-f8.fis - while_stepping
* monitors for failure under pillar centre line in stabilising
```

```
pillars
* run automatically during RELAX in ss-ref.d6k (whole run
under RELAX)
* sets fail2 = 1 the first time ff is detected
* RELAX in zonkd6k.fis checks for fail2 = 1 ==> does sav file
ca found-f8.fis
ca top_clos.fis ; monitors avg closure at top of model
set height = 320
hi top_clos
hi top_strn
ca pillstrn.fis ; avg axial strain of pillar
set stope_width=1.8
hi pillstrn
* ca zonkd6k.fis
* RELAX factor is taken to be uniform again
* modify to SOLVE FORCE=.1E6 at each big step (instead of
n_small_steps)
* do sav files according to no. of big_steps given in table 4
* do tmp sav file after each big_step
* remove sxx, syy forces at pillar side wall-creates false
confinement
table 4 1,250 2,500 3,625 4,750 5,875 6,1000
ca zonkd6k.fis
set n_big_steps 1000
set i1 33 i2 130 j1 1 j2 6
zonk
relax
```

fish files PILL-APS.FIS, FOUND-F8.FIS, TOP_CLOS.FIS and PILLSTRN.FIS are listed above fish file ZONKD6K.FIS is the same as ZONKD6M.FIS listed above, except that the names of the save filenames change accordingly. ◆

Spotlight

Spotlight on Infacon 8 in Beijing

INFACON (The International Ferroalloys Congress) was initiated by the SAIMM, FAPA and Mintek in1974. The congress rotates venues from Africa to Europe, Asia, South and North America and then back to Africa. Infacon 8 in Beijing is the second time the Congress has been held in Asia, the first being Infacon 3 in 1983 in Tokyo, Japan. Infacon 8 was organized by the Chinese Society for Metals and was held from June 7-10, 1998. As is usually the case many of the delegates were from the host country. However, attendance from 36 countries outside China made this the most widely attended Infacon to date. Forty delegates from South Africa made good use of the opportunity to not only attend the many interesting social and stimulating technical events but also to network with their counterparts from around the world.

A very comprehensive technical programme was compiled and the Congress proceedings were issued at registration in both English and Chinese. Papers were presented in parallel sessions and covered the following topics: Environmental, Silicon Metal and Ferrosilicon, Simulation, Control and Modelling, Chromium Metal and Ferrochromium, Ferromanganese. The opening plenary session dealt with Developments in Technology for Ferrochromium Production and was presented by Dr Aidan Edwards of Mintek and with Strategic Issues in the Ferroalloy Industries and was presented by Chris Stobart from the UK. The closing plenary session included presentations of the major producers and consumers namely China, South Africa, North America, Europe and Japan. There were 16 papers delivered by South African presenters during the plenary and technical sessions, the largest contingent outside China which indicates the considerable level of technical development work still going on in our local ferro-alloy industry. The funds generated from INFACON 6 in Cape Town in 1992 have supported research and development projects in the field of ferro-alloys at several universities in South Africa over the past eight years. The object of furthering science and technology and publishing papers on ferro-alloys at subsequent Infacon congresses has been met. The remaining funds have been awarded to the School of Process and Materials Engineering at the University of the Witwatersrand to support specific ferro-alloy projects declining with the recovery of ferrochromium and ferromanganese alloys and injection and mixing for ferro-alloy refining. Papers on the above were presented at Infacon 8.

Mintek has performed the function as the secretariat of the International Committee on Ferroalloys (ICFA) since 1974. Dr Aidan Edwards who has chaired ICFA since 1986 has handed the reins over to Dr Nic Barcza who in turn has stepped down as Secretary General. Tom Curr, Manager of Mintek's Pyrometallurgy Division has taken over this position. These changes were unanimously ratified at the ICFA meeting during Infacon 8 where the decision to hold the next Infacon namely Infacon 9 in North America was made. Quebec City was proposed as a probable venue in 2001 subject to approval by the North American Ferro Alloys Producers Association. Infacon 10 is provisionally scheduled for Zimbabwe in 2004 subject to finalization during Infacon 9 and the SAIMM will no doubt once again play a pivotal role in this prestigious event. ◆

Professional Directory

This could be your Professional Directory Advertisement

The South African Institute of Mining and Metallurgy
Founded in 1894

- 85 mm wide x 45 mm deep • R300 per insertion
- R1200 for six insertions paid in advance
- Logo can be included

For your bookings contact the Journal Secretary,
The South African Institute of Mining and Metallurgy
13th Floor, Cape Towers, 11–13 MacLaren Street, Johannesburg, 2001.
P.O. Box 61127, Marshalltown, 2107.
Tel: (011) 834-1273/7, Fax: (011) 838-5923

Geostokos Limited
Specialists in ore reserve estimation
Allan Business Centre, Whins Road, Alloa, Central Scotland FK10 3SA
Tel/Fax: 44 1259 217 914 e-mail: geo@stokos.demon.co.uk
http://www.stokos.sfan.com.br
In Southern Africa tel/fax: Dr Isobel Clark at 27 11 726 8729
e-mail: stokos@netactive.co.za

The South African Institute of Mining and Metallurgy
Founded in 1894

OBITUARY

		Date of Election	Date Deceased
I.S. Van Eyssen	Retired Associate	12 August 1938	1998
A.C. Petersen	Retired Fellow	14 March 1941	25 July 1998
L.A.L. Forder	Retired Fellow	12 April 1938	1 August 1998

SAIMM DIARY

MINING

COLLOQUIUM
Water Legislation
19 November 1998, Randfontein Estate Club, Randfontein

COLLOQUIUM
Simrac
19 November 1998, Witbank Civic Centre
24 November 1998, Goldfields Training Centre

METALS TECHNOLOGY

SCHOOL
Physical metallurgy
POSTPONED—Venue and date to be advised

INTERNATIONAL CONFERENCES

Extraction Metallurgy Africa '98
5–6 November 1998, Indaba Hotel, JOHANNESBURG

Fragblast 6
8–12 August 1999, Sandton Sun and Towers, Intercontinental JOHANNESBURG

Heavy Minerals Conference '99
1–3 November 1999, DURBAN

For further information, please contact:
The Secretariat, SAIMM, P.O. Box 61127, MARSHALLTOWN 2107
Tel.: (011) 834-1273/7, Fax: (011) 838-5923 or 833-8156, e-mail: saimm@tradepage.co.za